nature medicine

Human antibody repertoire after VSV-Ebola vaccination identifies novel targets and virus-neutralizing IgM antibodies

Surender Khurana[1], Sandra Fuentes[1], Elizabeth M Coyle[1], Supriya Ravichandran[1], Richard T Davey Jr[2] & John H Beigel[3]

Development of an effective vaccine against Ebola virus is of high priority. However, knowledge about potential correlates of protection and the durability of immune response after vaccination is limited. Here, we elucidate the human antibody repertoire after administration of vesicular stomatitis virus (VSV)-Ebola vaccine at 3 million, 20 million and 100 million plaque-forming units (PFU) and homologous VSV-Ebola vaccine boost in healthy adult volunteers. Whole genome-fragment phage display libraries, expressing linear and conformational epitopes of Ebola glycoprotein (GP), showed higher diversity of antibody epitopes in individuals vaccinated with 20 million PFU than in those vaccinated with 3 million or 100 million PFU. Surface plasmon resonance kinetics showed higher levels of GP-binding antibodies after a single vaccination with 20 million or 100 million PFU than with 3 million PFU, and these correlated strongly with neutralization titers. A second vaccination did not boost antibody or virus neutralization titers, which declined rapidly, and induced only minimal antibody affinity maturation. Isotype analysis revealed a predominant IgM response even after the second vaccination, which contributed substantially to virus neutralization *in vitro*. These findings may help identify new vaccine targets and aid development and evaluation of effective countermeasures against Ebola.

The recent 2014 epidemic of highly pathogenic Ebola virus (EBOV) in Western Africa has resulted in more than 28,652 human cases and 11,325 deaths (case fatality rate ~40%) as of 13 April 2016 (ref. 1). With occasional small outbreaks of new cases in Western Africa and the possibility of long-term persistence of virus in some survivors, it is feared that future outbreaks could occur and lead to severe epidemics. Therefore, development of an effective vaccine against Ebola is a high priority, both for pre-epidemic preparedness and for rapid vaccination to control future outbreaks[2]. Multiple vaccine candidates that have been shown to be protective against lethal challenge in preclinical nonhuman primate (NHP) models are currently in clinical trials[3–10]. Protection against EBOV disease is attributed, at least partially, to the humoral immune response, as passive transfer of antibodies to naive NHPs can protect recipients against lethal EBOV challenge[11–14]. Diverse ELISA, EBOV neutralization tests and immune parameters have been used to identify the vaccine correlates of protection[15–17]. A recent study also investigated the role of T cells in EBOV-infected patients and found that expression of the inhibitory molecules cytotoxic T lymphocyte-associated protein 4 (CTLA-4) and programmed cell death protein 1 (PD-1) on $CD4^+$ and $CD8^+$ T cells was lower in survivors than in fatal cases[18]. However, to date, no single assay has been found to be predictive of protection, and the correlation of antibody titers measured by various assays has not been clearly demonstrated. Coupled with the difficulty of conducting adequate randomized controlled trials to demonstrate vaccine effectiveness on the basis of clinical EBOV disease, it is important to identify and understand immune markers that are reasonably likely to predict clinical benefit and can facilitate evaluation of vaccine candidates[19,20].

Recently, a recombinant VSV (rVSV)-based vaccine expressing Ebola Zaire surface glycoprotein from the Kikwit 1995 strain (rVSVΔG-ZEBOV-GP) was reported to decrease transmission to close contacts in a ring vaccination study in Guinea[3]. Here we performed an in-depth comprehensive analysis of the humoral immune response after primary rVSVΔG-ZEBOV-GP vaccination administered at 3 million, 20 million or 100 million PFU and homologous rVSVΔG-ZEBOV-GP vaccine boost in healthy US adult volunteers in a phase 1 placebo-controlled trial[8]. Polyclonal serum was analyzed quantitatively and qualitatively to elucidate antibody epitope repertoires using gene-fragment phage display libraries (GFPDLs) and surface plasmon resonance (SPR) technology to measure real-time antibody binding kinetics, antibody cross-reactivity, immunoglobulin isotypes, affinity maturation and antibody persistence in recipients of the rVSVΔG-ZEBOV-GP vaccine. Previously, GFPDLs spanning the entire genome of highly pathogenic avian influenza virus were used to map the antibody repertoires of convalescent sera from H5N1-infected individuals and recipients of pandemic influenza vaccinations, which revealed several diagnostic and protective targets[21–23].

[1]Division of Viral Products, Center for Biologics Evaluation and Research (CBER), US Food and Drug Administration, Silver Spring, Maryland, USA. [2]National Institute of Allergy and Infectious Diseases, National Institutes of Health, Bethesda, Maryland, USA. [3]Leidos Biomedical Research, Inc., Frederick National Laboratory for Cancer Research, Frederick, Maryland, USA. Correspondence should be addressed to S.K. (surender.khurana@fda.hhs.gov).

Received 17 June; accepted 12 September; published online 31 October 2016; corrected online 15 November 2016; doi:10.1038/nm.4201

RESULTS

Antibody epitope repertoire after vaccination

A rVSVΔG-ZEBOV-GP vaccine was administered intramuscularly at 3 million, 20 million or 100 million PFU to 39 healthy adult volunteers at the US National Institute of Allergy and Infectious Diseases (NIAID). In each dosing cohort, ten people received active vaccine, and three received a saline placebo. Serum samples from each individual were collected before vaccination (day 0), after the first vaccination (day 28), after the second vaccination (days 42 and 56) and on days 84 and 180. To analyze the epitope repertoire of serum samples from participants who received the rVSVΔG-ZEBOV-GP vaccine, we generated a GFPDL containing 50- to 1,000-bp fragments of the *GP* gene from the EBOV Mayinga strain (**Supplementary Fig. 1**) or the homologous Kikwit strain (**Supplementary Fig. 2**), with $>10^7$ unique phage clones. These were expected to display all possible linear and conformational epitopes. The GP sequence of Mayinga of 1976 differs from the Kikwit strain of 1995 used in the vaccine by only nine amino acids, whereas the Makona strain of 2014 differs from Mayinga by 20 amino acids (**Supplementary Fig. 2**).

Sequencing of the EBOV GFPDL confirmed a random distribution of size and sequence of inserts that spanned the entire GP (**Supplementary Fig. 3**). To ascertain that the antibody repertoire identified using the GFPDL approach represented both linear and conformational epitopes, we performed two independent experiments. First, a panel of EBOV-protective monoclonal antibodies (MAbs) was used to identify and confirm the potential of the EBOV GFPDL to map both linear and conformational antibody epitopes. This panel included 6D8 and 13F6, which are components of the MB-003 cocktail for treatment of EBOV infection (**Supplementary Fig. 4**), and conformation-dependent cross-reactive neutralizing and protective human MAbs derived from EBOV survivors[24] (**Supplementary Fig. 5**). The consensus epitope sequences obtained through GFPDL analysis were similar to the footprints previously identified for the MB-003 MAbs[25,26] or for MAbs from survivors[24], providing proof of concept that the GFPDL approach can identify linear and conformation-specific antibodies in polyclonal serum after EBOV infection or vaccination.

Second, we determined the capacity of the EBOV GFPDL to adsorb EBOV GP-specific antibodies in post-vaccination polyclonal human sera. After two rounds of adsorption with the EBOV GFPDL, 85–92% of GP-specific antibodies in post-vaccination human sera were adsorbed by GP phage display libraries, as determined by binding to EBOV GP in ELISA (**Supplementary Fig. 6**). Together, the epitope mapping of MAbs and adsorption studies in post-vaccination polyclonal sera provided support for using the EBOV GP GFPDL to dissect the polyclonal antibody repertoires in human sera.

To study antibody responses after rVSVΔG-ZEBOV-GP vaccination, we collected serum specimens from individuals vaccinated with 3 million, 20 million or 100 million PFU vaccine or placebo control before vaccination (day 0), 28 d (day 28) after the primary vaccination and 28 d after booster vaccination (day 56). The sera of all participants in each dose group were pooled and used for mapping of overall antibody epitope repertoires by EBOV GFPDL (**Fig. 1**).

Prevaccination sera and the placebo controls were bound by very few phages. In the rVSVΔG-ZEBOV-GP-vaccinated groups, 4 weeks after the first vaccination, the number of bound phages was higher in sera from the 20-million-PFU dose (2.12×10^6) group than in sera from the 3-million-PFU and 100-million-PFU groups (1.12×10^6 and 1.45×10^6 phages, respectively) (**Fig. 1a**). Sequencing of GP fragments expressed by phages bound with sera after the first vaccination showed a high frequency of bound phages displaying both small and large fragments mapping across the N-terminal GP1 head domain and, to a lesser degree, the C-terminal GP2 stalk domain of the EBOV GP protein (**Fig. 1b**). Sera from the 3-million-PFU and 20-million-PFU cohorts contained antibodies that mapped to the glycan cap and mucin domain and that recognized an epitope in the transmembrane region of the GP2 protein that was not captured by sera from the 100-million-PFU dose cohort. Sera from the 20-million-PFU dosing cohort additionally recognized several small and large immunodominant epitopes in the N-terminal half of EBOV GP mapping to the receptor-binding region (RBR) and between the RBR and the glycan cap domain (**Fig. 1b**).

Unexpectedly, after the second vaccination, the number of EBOV GFPDL bound phages decreased 2–10 times relatively to the first vaccination (**Fig. 1a**). The antibody epitope profiles did not substantially change, apart from an apparent reduction in antibodies mapping to the GP2 transmembrane region in the 3-million- and 20-million-PFU dose recipients, an increase in antibodies specific to the glycan cap in the 20-million-PFU cohort, and a small reduction in antibodies recognizing large sequences in the mucin-like domain from the 100-million-PFU group (**Fig. 1c**).

Antigenic sites within EBOV GP

EBOV-neutralizing and/or protective MAbs, such as KZ52 and the MAb cocktails ZMAb, ZMapp and MB-003, have been shown to recognize epitopes within or flanking the mucin-like domain, glycan cap or base of GP[25,26] (**Fig. 2a**). Vaccination with rVSVΔG-ZEBOV-GP generated an immune response to 19 unique antigenic sites defined by six large antigenic regions (herein referred to as GP-I through GP-VI) and 13 smaller antigenic sites (GP-II.1 through GP-V.7) contained within EBOV GP (**Fig. 2a** and **Supplementary Table 1**). These antigenic regions and sites include several novel linear and conformational epitopes, including GP-II, GP-II.1, GP-II.2, GP-IV.1, GP-IV.3, GP-V.1, GP-V.4, GP-V.5, GP-V.6, GP-V.7 and an immunodominant sequence (GP-VI) in the transmembrane or cytoplasmic tail. The frequency of phages expressing these GP antigenic sites selected by sera after the first (**Fig. 2b**) and second (**Fig. 2c**) vaccinations for the three rVSVΔG-ZEBOV-GP dose groups are shown in **Supplementary Table 1**. Antibodies in post-vaccination sera from the 20-million-PFU dose group showed the highest epitope diversity, as assessed by selecting phage clones from most of the

Figure 1 Analysis of antibody repertoires elicited in adults after first and second vaccinations with different doses of rVSVΔG-ZEBOV-GP. (**a**) Number of captured phage clones isolated using EBOV GFPDL affinity selection with sera from adults after the first and second vaccinations with 3 million, 20 million or 100 million PFU rVSVΔG-ZEBOV-GP vaccine ($n = 10$ per group). (**b**,**c**) Schematic alignments of the peptides recognized in sera after the first (**b**) and second (**c**) vaccinations, identified by panning with EBOV GFPDL. Amino acid designations are based on the GP protein sequence encoded by the complete EBOV *GP* gene (**Supplementary Fig. 1**). SP, signal peptide; HR1, heptad repeat 1; HR2, heptad repeat 2; TM, transmembrane domain; CT, cytoplasmic tail. Bars indicate identified inserts in GP sequence. Graphical distribution of representative clones with a frequency of ≥2 obtained after affinity selection are shown. The horizontal positions and the lengths of the bars indicate the peptide sequence displayed on the selected phage clone to its homologous sequence in the EBOV GP sequence on alignment. The thickness of each bar represents the frequency of repetitively isolated phage, with the scale shown below the alignment. The GFPDL affinity selection was performed in quadruplicate (two independent experiments by two different investigators, who were blinded to sample identity).

antigenic sites within GP, whereas the sera from the lower (3 million PFU) and higher (100 million PFU) dose groups contained antibodies that predominantly mapped to the C-terminal half of the EBOV GP.

The surface exposure of each of these antigenic sites on the EBOV GP crystal structure[27] (PDB 3CSY; includes GP residues 33–189, 214–278, 299–310 and 502–599) and the model of complete EBOV

a

	3 10^6 PFU		20 10^6 PFU		100 10^6 PFU	
	Post-1st	Post-2nd	Post-1st	Post-2nd	Post-1st	Post-2nd
Phage titer	1.12 10^6	1.8 10^5	2.12 10^6	1.45 10^6	1.45 10^6	8.40 10^5

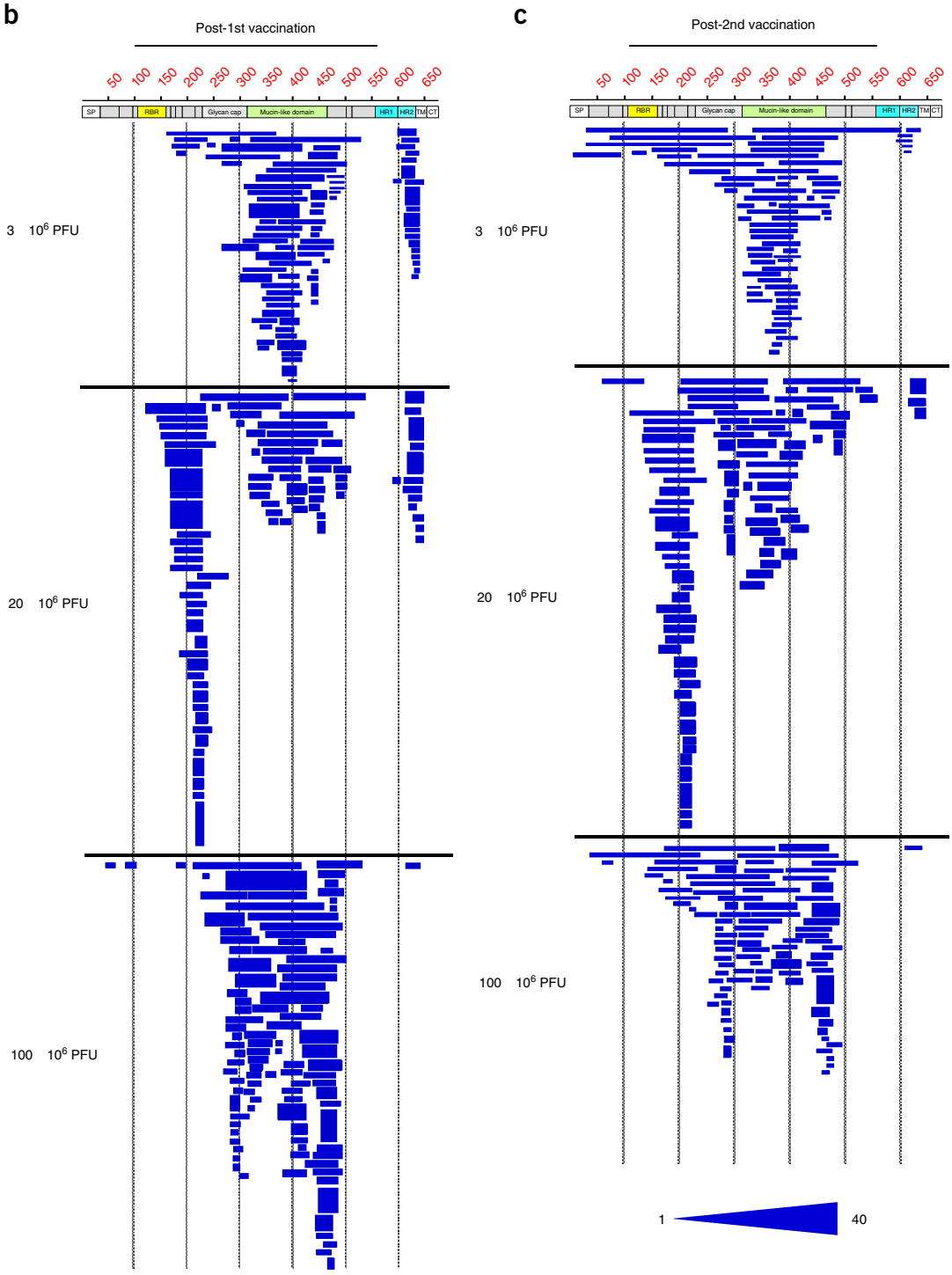

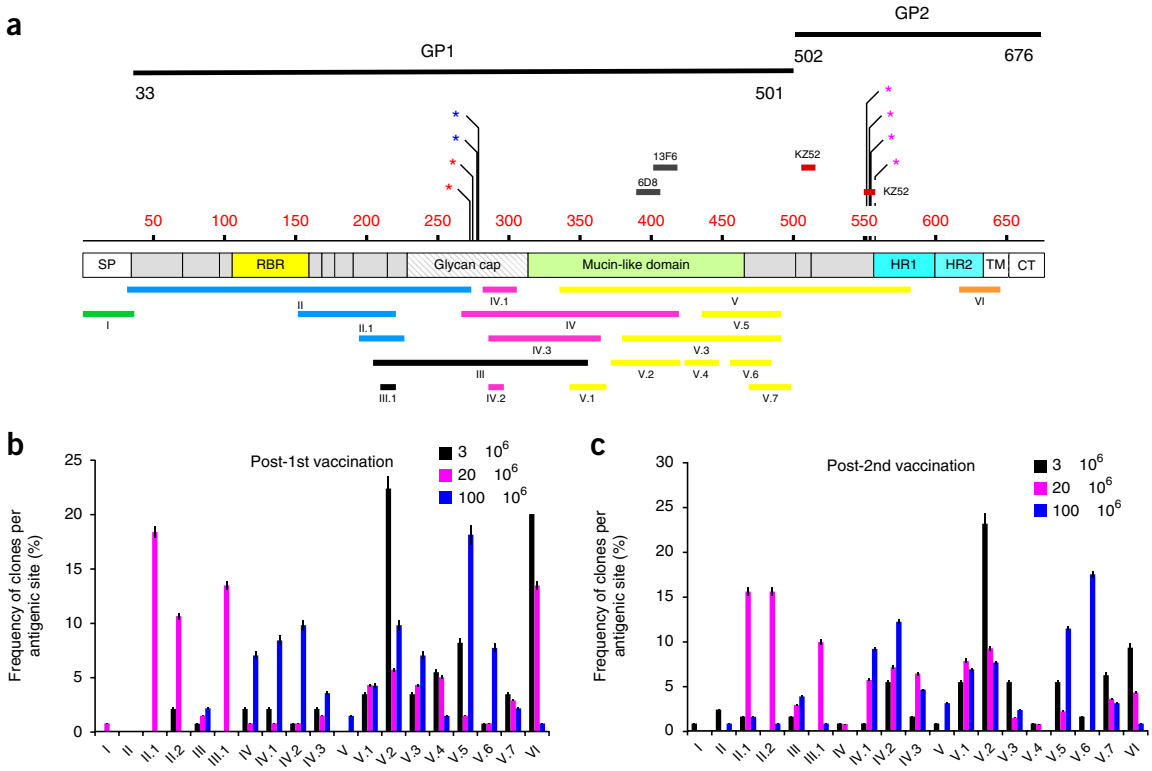

Figure 2 Elucidation of antibody epitope profile against Ebola GP after rVSVΔG-ZEBOV-GP vaccination in humans. (**a**) Antigenic sites within the EBOV GP recognized by serum antibodies after vaccination (based on data presented in **Fig. 1**). Amino acid designations are based on the GP protein sequence encoded by the complete EBOV *GP* gene (**Supplementary Fig. 1**). Epitopes previously described using MAbs are shown above the GP schematic. Critical residues for binding of MAbs in anti-EBOV cocktails ZMAb (1H3 (blue asterisks) and 2G4 and 4G7 (pink asterisks)), MB-003 (13C6 (red asterisks), 6D8 and 13F6) and MAb KZ52 (ref. 25) are shown. (**b**,**c**) Distribution and frequency of phage clones expressing each of the key GP antigenic sites after first (**b**) or second (**c**) vaccination across dosage groups (3 million PFU, 20 million PFU and 100 million PFU). The number of clones encoding each antigenic site was divided by the total number of EBOV GFPDL-selected clones for pooled sera from each vaccine-dose group and represented as a percentage. Error bars represent s.e.m. of 4 independent experiments. The GFPDL affinity selection was performed in quadruplicate.

GP monomer[28] (**Supplementary Fig. 7**) are shown in **Figure 3**. The surface representation showed that most of the key antibody targets of rVSVΔG-ZEBOV-GP, including several of the GP epitopes (GP-II, GP-II.1, GP-II.2, GP-IV.1, GP-IV.3, GP-V.1, GP-V.4, GP-V.5, GP-V.6, GP-V.7) discovered in this study, are exposed on the native ZEBOV GP structures. Analysis of sequence homology of GP showed that some sites, including GP-II, GP-II.1, GP-IV.1, GP-IV.2 and GP-VI, are >70% conserved between diverse EBOV strains, such as Sudan, Bundibugyo, and Kikwit (**Supplementary Table 2**). These data suggest that antibodies induced after rVSVΔG-ZEBOV-GP vaccination against some conserved antigenic sites may cross-react with diverse EBOV strains, even though cross-protection has not been observed in rVSVΔG-ZEBOV-GP-vaccinated NHPs challenged with EBOV Sudan virus[29].

Correlation of GP antibody binding with EBOV neutralization

Because the GFPDL analyses were carried out on the pooled serum samples from each group, we performed quantitative and qualitative analyses of individual pre- and post-vaccination sera with recombinant glycosylated GP produced in a mammalian system using an SPR-based real-time kinetics assay.

Binding kinetics of individual serum samples from the three vaccine-dose cohorts at early post-vaccination time points (28 d after first vaccination and 14 and 28 d after second vaccination) and at later time points (day 84 and day 180) was performed using the GP from Mayinga and Makona strains (**Fig. 4a**,**b**). Antibody binding titers of individual serum samples ($N = 10$ for each vaccine group at each time point) against GP were measured as resonance units (RU) in SPR (**Fig. 4**). Control sera from placebo did not show significant antibody binding to GP before or after mock vaccination. After the first rVSVΔG-ZEBOV-GP vaccination (day 28), all samples reacted strongly with GP from Mayinga (**Fig. 4a**) and Makona strains (**Fig. 4b**), with sera from the 20-million- and 100-million-PFU groups showing higher binding (mean RU = 2,152 and 2,056, respectively) than those of the 3-million-PFU group (mean RU = 1,197), but the difference among groups did not reach statistical significance. However, the mean serum antibody reactivity decreased marginally (mean RU = 800 for 3 million PFU; 1,608 for 20 million PFU; 1,715 for 100 million PFU) for all the vaccine dose groups by day 42 (14 d after the second vaccination) and even further by day 56 (28 d after administration of the homologous boost; mean RU = 679 for 3 million PFU; 1,409 for 20 million PFU; 1,536 for 100 million PFU). By days 84 and 180, serum anti-GP titers had diminished substantially, such that by day 180, 80% of individuals had very weak GP-binding antibody levels for all vaccine groups, though binding-antibody titers were marginally higher for the group that received the highest vaccine dose (mean GP binding RU = 133 for 3 million PFU; 260 for 20 million PFU; 490 for 100 million PFU). We observed a strong correlation between *in vitro* EBOV neutralization titers (**Fig. 4c**) and the titers of serum GP-binding antibody, as measured by SPR, after rVSVΔG-ZEBOV-GP vaccination ($r = 0.75$; $P < 0.0001$) (**Fig. 4d**). This analysis revealed that the replicating

rVSVΔG-ZEBOV-GP vaccination generated strong GP-binding antibodies that peaked after the first vaccination but were not boosted after the second vaccination and were not long lasting.

Antibody affinity maturation after vaccination

To further investigate whether different rVSVΔG-ZEBOV-GP vaccine doses promote anti-GP affinity maturation, we determined the

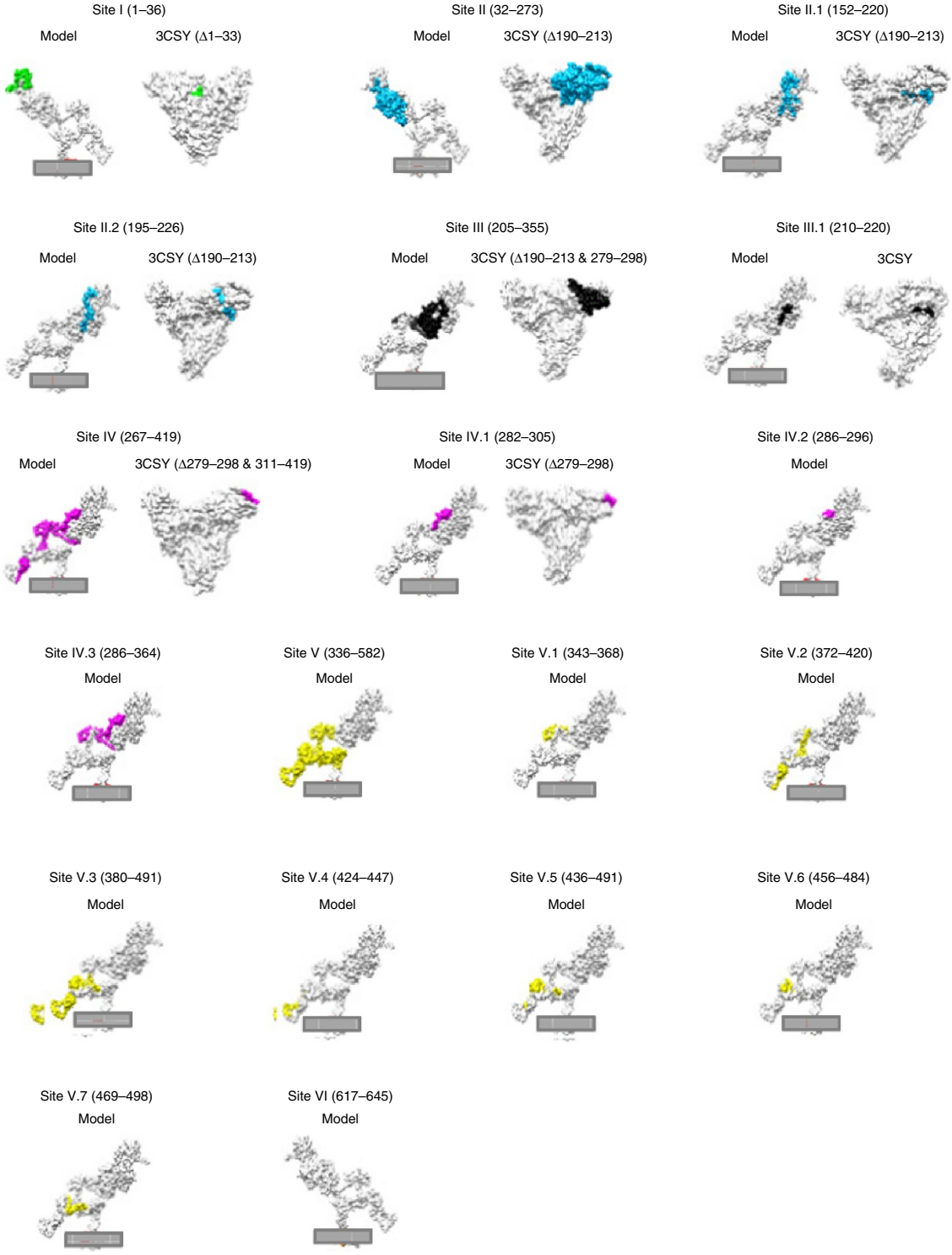

Figure 3 Structural representation of antigenic sites in EBOV GP identified with GFPDL. Representations of individual antigenic sites on the surface structures of a complete EBOV GP model (left) and solved EBOV GP structure (PDB 3CSY)[27] are shown (right) where available; antigenic sites in a monomer (chain A) are color coded as in **Figure 2**. The EBOV GP structure used for crystallography encompasses amino acid residues 33–189, 214–278, 299–310 and 502–599 of the mature 676-aa GP sequence. The transmembrane (TM) domain is shown in orange, and the viral membrane is shown (gray bar) on the model images. Sites I, II and VI on the model are shown in front view. Sites II.1, II.2, III, III.1, IV, IV.1, IV.2, IV.3, V and V.1–V.7 are shown in rear view. All sites (except site I) are depicted in front view on the solved structure.

dissociation rates (K_d) of post-vaccination serum antibody–antigen complexes using SPR. Dissociation rate is independent of antibody concentration and provides a measurement of overall affinity of polyclonal antibody binding, as previously described[23]. The off-rates for polyclonal serum antibodies bound to GP were lower (indicating stronger affinity) at 14 d and 28 d after the second vaccination than at

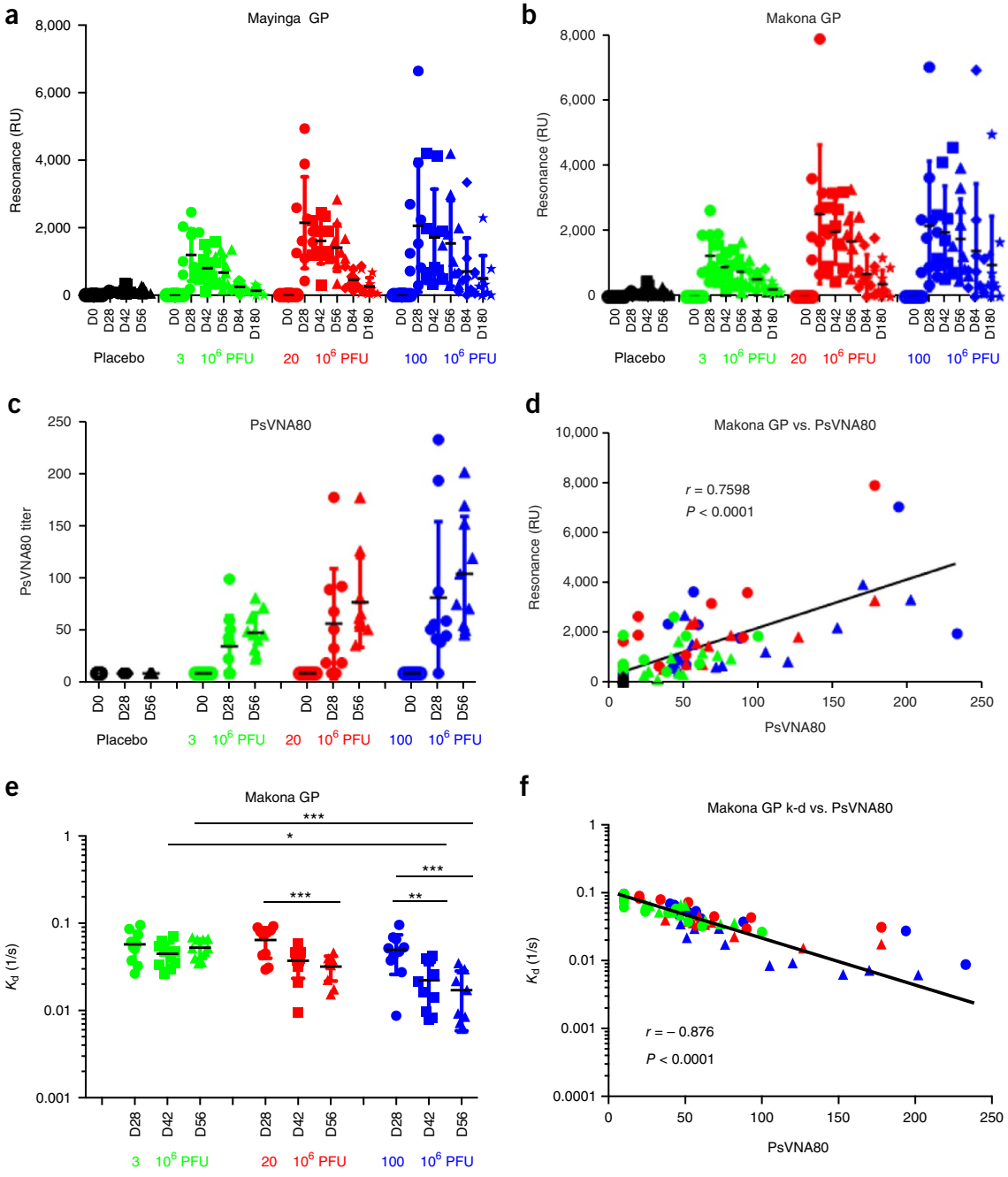

Figure 4 SPR-based analysis of sera from rVSVΔG-ZEBOV-GP-vaccinated individuals with EBOV GP purified protein. (**a**,**b**) Total binding (RU) to purified mature GP from Mayinga (**a**) or Makona (**b**) EBOV strains in serum samples collected at different time points from adults receiving vaccine or placebo intramuscularly on day 0 (D0) and day 28 (D28). Maximum RU values for GP binding by serum antibodies obtained from all individuals are shown. Data are mean ± s.d. No significant differences were found between groups ($P \geq 0.05$, multiple-comparison adjustment using Bonferroni method). (**c**) EBOV neutralization endpoint titers of serum antibodies in pseudovirus neutralization assay (PsVNA) used for EBOV GFPDL-based epitope mapping. PsVNA80 titer refers to the highest serum dilutions required to achieve 80% viral inhibition. (**d**) Correlation between maximum RU for post-vaccination sera against Makona GP and homologous virus neutralization titers (PsVNA80; Spearman $r = 0.7598$, $P < 0.0001$) after the first (day 28) and second (day 56) vaccinations. (**e**) Polyclonal antibody affinity to EBOV GP after rVSVΔG-ZEBOV-GP vaccination. SPR analysis of post-vaccination sera was performed with Makona GP to determine the K_d of polyclonal serum antibodies from all individuals at different post-vaccination time points (Online Methods). Horizontal bars indicate mean values. $^*P < 0.05$; $^{**}P < 0.01$; $^{***}P < 0.001$. (**f**) Correlation of GP-binding affinity, as measured by K_d of post-vaccination human polyclonal antibodies against Makona GP, with the homologous virus neutralization titers (PsVNA80; Spearman $r = 0.876$, $P < 0.0001$) after the first (day 28) and second (day 56) vaccinations. All SPR experiments were performed twice.

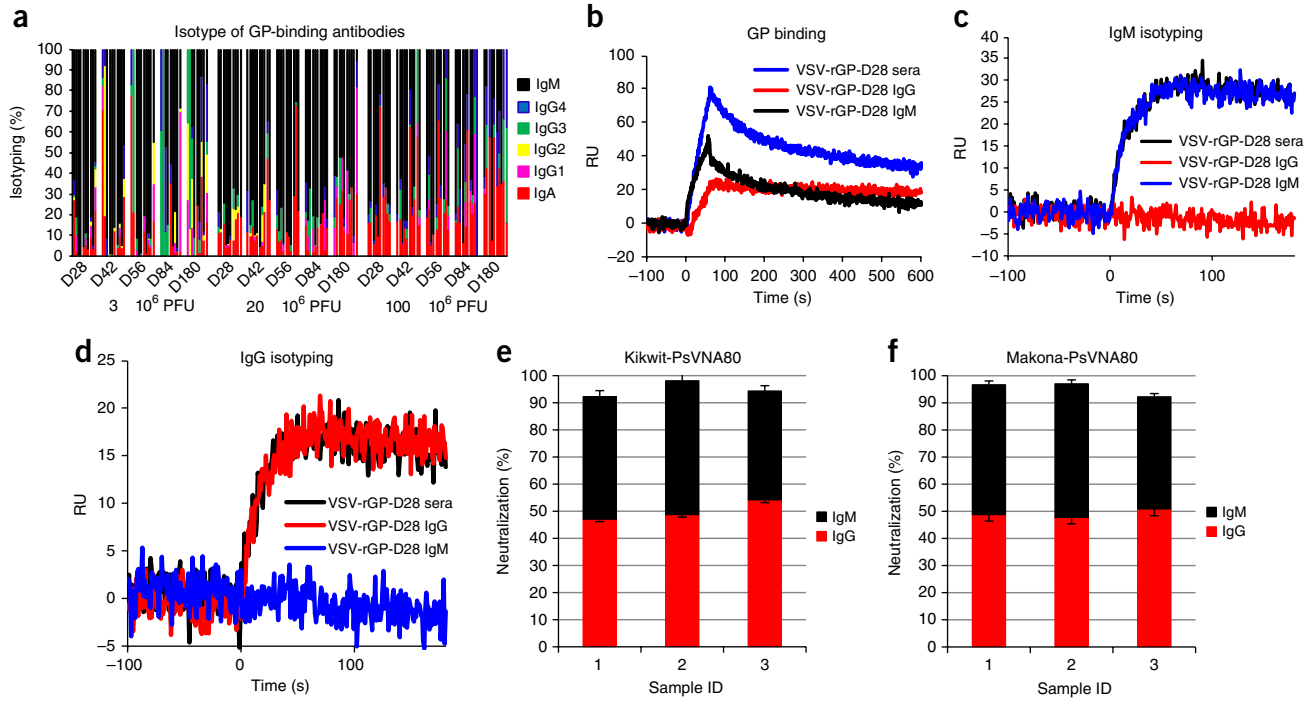

Figure 5 Antibody isotypes in human serum binding to EBOV GP after vaccination and the role of IgM antibodies in virus neutralization. (**a**) Isotypes of serum antibodies bound to EBOV GP for samples collected from adults from each of the three vaccine-dose groups at different time points, as measured in SPR. RU values for each anti-GP antibody isotype were divided by the total combined RU value for all isotypes for individual serum samples and represented as a percentage. (**b**) GP binding of IgG and IgM fractions purified from day 28 (VSV-rGP-D28) sera of one of the three subjects with equivalent representations of IgG and IgM isotypes in the EBOV GP-bound antibodies. (**c**,**d**) Confirmation of the purity of isotype binding to GP using anti-human IgG (**c**) and anti-human IgM (**d**) secondary antibodies. (**e**,**f**) Pseudovirus neutralization assay to evaluate purified IgG and IgM antibodies for virus neutralization against Kikwit (**e**) and Makona (**f**) EBOV strains. The data are represented as the relative contributions of IgM and IgG antibodies to the total neutralization observed for each sample. Error bars represent mean ± s.e.m. of 2 technical replicates. All SPR experiments were replicated twice.

28 d after the first vaccination, but this difference reached statistical significance only for the 20-million-PFU and 100-million-PFU groups (**Fig. 4c**). However, polyclonal antibody off-rates ($K_d = 10^{-2}$–10^{-3}/s) were low, even after two vaccinations, compared to some other human viral vaccines[23]. GP-specific antibody off-rates after the first (day 28) and second vaccination (day 56) correlated strongly with virus neutralization titers ($r = -0.876$, $P = <0.0001$), emphasizing the potential importance of antibody affinity maturation for antiviral activity (**Fig. 4f**). These observations suggest that the higher rVSVΔG-ZEBOV-GP vaccine doses (20 million PFU and 100 million PFU) promote better antibody affinity maturation to GP than the lower vaccine dose.

Anti-GP isotype and EBOV-neutralizing capacity

Isotype analysis of the GP-binding antibodies demonstrated representation of all isotypes (IgA, IgG and IgM) and IgG subclasses in post-vaccination sera (**Fig. 5a**). We were surprised to find that most of the GP-binding antibodies both after primary and after booster vaccinations, were of IgM isotype in all vaccine-dose groups (**Fig. 5a**). The second most abundant GP-binding antibodies were of IgA isotype, and their frequency in serum increased with dosage (mean IgA = 4% for 3 million PFU; 10% for 20 million PFU; 20% for 100 million PFU) at day 56. The anti-GP isotype reactivity was also analyzed by ELISA (**Supplementary Fig. 8**). Antibody isotyping of GP-binding antibodies in post-vaccination sera by ELISA showed concordance with the isotypes determined by SPR, but ELISA underestimated the proportion of GP-binding IgM antibodies compared to SPR. In contrast, at later time points (day 84 and day 180) after vaccination, the GP-binding antibodies remaining in the sera (**Fig. 4a**) were of IgA or IgG subclasses (**Fig. 5a**), suggesting that most of the anti-GP antibody response generated early after vaccination is of the IgM isotype, which does not provide a long-lasting systemic anti-GP antibody response. After vaccination, of the total GP-bound IgG antibodies, IgG1, IgG2 and IgG3 contributed most to GP binding in the 3-million-PFU and 20-million-PFU vaccine cohort, whereas for the 100-million-PFU dose a significant amount of anti-GP antibodies were of IgG3 and IgG4 subclasses (**Supplementary Fig. 9**).

To understand the functional role of IgM antibodies in the post-vaccination response, we evaluated their contribution to virus neutralization and compared them to IgG antibodies in post-vaccination sera. We used anti-human IgG and anti-human IgM affinity chromatography columns to purify IgG and IgM antibodies from three sera samples, taken after the second vaccination, that showed similar amounts of GP-binding IgG and IgM antibodies and evaluated binding to the GP in SPR (**Fig. 5b**), isotype specificity (**Fig. 5c**,**d**) and virus neutralization of Kikwit and Makona EBOV strains (**Fig. 5e**,**f**). The IgG/IgM ratio determined from affinity chromatography in post-vaccination sera was in good agreement with that determined by SPR. The purified IgG and IgM antibodies from all sera reacted with GP, and, as expected, the IgG antibodies showed higher affinity (slower dissociation) to GP than IgM in SPR (**Fig. 5b**). The purity of antibody isotypes was confirmed by human IgG– and human IgM–specific secondary antibodies using SPR (**Fig. 5c**,**d**). The purified post-vaccination IgM antibodies at serum concentration levels contributed 40–50% to virus neutralization, and these results were similar to those with IgG antibodies purified from post-vaccination sera from the same individuals (**Fig. 5e**,**f**). These results suggest that anti-GP IgM antibodies could have an important role in protection against EBOV disease *in vivo*.

The results of our study demonstrate independent evolution of antibody binding patterns to EBOV GP—in terms of epitope repertoire diversity, affinity maturation and isotype switching—in the three vaccine-dose groups after the first and second vaccinations and show an important contribution of anti-GP IgM antibodies to EBOV neutralization.

DISCUSSION

In-depth understanding of the humoral immune response to Ebola vaccines under advanced development is required to identify meaningful correlates of protection in humans and animal models to facilitate evaluation of effective vaccine candidates[20]. The epitope-binding patterns in the GP antigenic sites were most diverse in the 20-million-PFU dose samples. This effect, in which a more diverse antibody repertoire is generated from a lower vaccine dose, has been observed in multiple human influenza vaccination studies and was linked with optimal $CD4^+$ T cell help, which may affect the B cell and T cell response differently after vaccination[30–33]. The lower numbers of captured GFPDL phages after the second vaccination, as compared to the first vaccination, suggest that pre-existing antibodies against rVSVΔG-ZEBOV-GP after the first vaccination may have impeded replication of the rVSV vector and possibly masked some GP epitopes. Notably, the 20-million-PFU dose, selected for the phase 2/3 clinical trials in Western Africa on the basis of safety and *in vitro* neutralization data, generated the broadest antibody repertoire after vaccination. These findings in US adults (including equal numbers of white and black participants) should be expanded in future studies in populations from various geographic regions, such as Western Africa, to determine whether post-vaccination antibody profiles differ between people of European and African ancestry and how they compare with EBOV survivors. The immune markers identified in this study should be further investigated for their association with protection in animals and humans. After finding that a substantial proportion of anti-GP antibodies were of IgM and IgA isotypes, we performed GFPDL analysis to determine specific epitopes recognized by IgA, IgG and IgM antibodies in post-vaccination sera. In the sera pooled from each group after the first vaccination, the number of bound phages was approximately twofold higher in IgM-bound antibodies than in protein A/G–bound (primarily IgG) antibodies, and in IgA-bound antibodies was about tenfold lower for all vaccine groups (**Supplementary Table 3**). We performed an additional analysis of sera from individuals in the 20-million-PFU and 100-million-PFU groups using IgA-, IgG- and IgM-specific capture beads to further define the fine epitope specificity of these antibodies after the first vaccination using homologous Kikwit GP EBOV strain GFPDL (**Supplementary Fig. 10**). The epitope repertoires of IgG-specific antibodies in individual post-vaccination sera were similar to those identified in IgG antibodies from pooled post-vaccination sera from the 20-million-PFU and 100-million-PFU dose groups (**Fig. 1**). However, the IgM antibody epitope repertoire in the 100-million-PFU dose group was more diverse than that of the 20-million-PFU group, which predominantly recognized the mucin-like domain. The individual IgM GFPDL responses quantitatively tracked the SPR data for total GP-binding antibodies, which measures binding of all anti-GP antibody isotypes. In both dose groups (20 million and 100 million PFU), IgA-specific polyclonal repertoire was more focused on the glycan cap and mucin-like domain, but sera from the 20-million-PFU group recognized the antigenic site V.7 at the C terminus of GP1 with higher frequency (**Supplementary Fig. 10**). One possible limitation of GFPDL-based assessment is that it is unlikely to detect paratopic interactions that require post-translational modification or rare quaternary epitopes that cross GP protomers. However, 85–92% of anti-GP antibodies from post-vaccination sera were removed by adsorption with the EBOV GP GFPDL, supporting the use of the EBOV GP GFPDL for analyses of human sera, as has been observed with other viral antigens, including different influenza strains, respiratory syncytial virus (RSV) protein F (RSV-F) and heavily glycosylated RSV-G[21–23,34]. Moreover, binding to properly folded glycosylated Ebola GP in SPR can overcome these limitations and provide additional insight into the post-vaccination anti-GP polyclonal antibody response. Real-time antibody kinetics of individual post-vaccination sera by SPR revealed several unexpected findings, including lack of impact of the second vaccination on anti-GP responses, a fast decay of anti-GP titers within 2 months after the second vaccination, limited antibody class switching and modest antibody affinity maturation.

The observation of low antibody class switching after rVSVΔG-ZEBOV-GP vaccination is notable. Our findings suggest that IgM antibodies are the predominant isotype and decayed rapidly after the first and second vaccination. Although IgM antibodies are of low affinity, their multivalency compensates for overall binding avidity and helps in virus neutralization. Therefore, IgM antibodies may contribute to protection against infection, which would explain the relatively rapid protection that has been described in NHP studies and the rVSVΔG-ZEBOV-GP ring vaccination study in Africa[3]. The amount of IgA in most post-vaccination sera samples was too low to purify and perform a reproducible EBOV neutralization assay. IgA purified from sera from two vaccine recipients showed that GP-specific IgA antibodies can neutralize virus *in vitro* but to a lesser extent than IgM antibodies.

Most ELISAs used for evaluation of Ebola vaccines measure predominantly anti-GP IgG antibody titers, because they rely on anti-human IgG secondary antibodies. Such ELISA titers alone may underestimate the full spectrum of the vaccine-induced immune response. Although incorporating an anti-human IgM secondary antibody in the ELISA may help mitigate this deficiency, the washing steps involved in the ELISA process, which are important to reduce nonspecific binding, may elute most of the low-affinity IgM antibodies. In addition, anti-GP IgA antibodies may contribute to protection against EBOV infection and disease *in vivo*, especially at mucosal surfaces. In contrast, the SPR approach captures all antibody classes, including IgM, IgA and IgG, and is also more appropriate for maintaining the native structure of EBOV GP and preserving conformational epitopes.

Class switching and antibody affinity maturation require continuous signals from T cells in the form of cytokines and comigration of antigen-specific follicular helper T cells and B cells into germinal centers in lymph nodes[35,36]. The influence of pre-existing rVSVΔG-ZEBOV-GP-specific antibodies or anti-VSV vector responses at the time of the booster vaccination, with their attenuating effects on rVSV replication and masking of GP epitopes, could adversely affect the formation of germinal centers and prevent antibody class switching, affinity maturation and durable response, as observed in previous vaccine studies[37,38]. A second vaccination or prime-boost with alternative vaccine platforms (including different VSV serotype vectors) could provide a meaningful increase in affinity maturation and a better immune response, as was observed in prime-boost H5N1 and H7 influenza vaccine studies in humans[37–40]. In these studies, it was observed that a 3-month minimum interval between the first and second vaccine doses was required for optimal neutralizing-antibody response and antibody affinity maturation.

In summary, we have demonstrated independent evolution of antibody immune responses—in terms of antibody epitope repertoire diversity, affinity maturation, durability and isotype switching—after vaccination with a live rVSV vector–based vaccine in three vaccine-dose groups and revealed the importance of a predominantly anti-GP IgM response for

EBOV neutralization. These findings could have significant implications for further development and evaluation of Ebola vaccines. Future Ebola vaccine studies should follow the rate of decay of anti-VSV antibodies to identify the time interval needed for a booster vaccination to generate optimal antibody affinity maturation and durable antibody responses. Our observations suggest that it is important to develop appropriate assays that can provide in-depth understanding of post-vaccination and post-infection antibody responses to help guide development and evaluation of effective Ebola countermeasures such as therapeutics and vaccines.

METHODS

Methods, including statements of data availability and any associated accession codes and references, are available in the online version of the paper.

Note: Any Supplementary Information and Source Data files are available in the online version of the paper.

ACKNOWLEDGMENTS

We thank S. Rubin and H. Golding for reviewing the manuscript and J. Voell, P. Munoz, R. McConnell, H. Baus, C. Rehm and J. Metcalf for help with clinical studies. We thank J. Crowe (Vanderbilt University) for the gift of MAb 289 and MAb 324. The clinical trial from which the test sera were derived was funded partly by the US National Institute of Allergy and Infectious Diseases. The antibody characterization work described in this manuscript was supported by FDA-MCMi-Ebola funds to S.K. The latter funders had no role in study design, data collection and analysis, decision to publish or preparation of the manuscript. This project was funded in whole or in part with federal funds from the US National Cancer Institute under contract HHSN261200800001E. The content of this publication does not necessarily reflect the views or policies of the US Department of Health and Human Services, nor does mention of trade names, commercial products, or organizations imply endorsement by the US government. We thank the US Army Medical Research Institute of Infectious Diseases team, including S. Kwilas, M. Wisniewski and J. Hooper, for providing the pseudovirion neutralization assay data used in this study. The pseudovirion work was funded by the US Department of Defense (DoD) Medical Countermeasures Systems' Joint Vaccine Acquisition Program at Fort Detrick, Maryland. The opinions, interpretations, conclusions and recommendations contained herein are those of the authors and are not necessarily endorsed by the US DoD.

AUTHOR CONTRIBUTIONS

S.K. designed research; S.F., S.R., E.M.C. and S.K. performed research; J.H.B. and R.T.D. conducted phase 1 study and contributed clinical samples; S.K., J.H.B. and R.T.D. contributed to writing the manuscript.

COMPETING FINANCIAL INTERESTS

The authors declare no competing financial interests.

1. Centers for Disease Control and Prevention. 2014 Ebola outbreak in West Africa—case counts. *Centers for Disease Control and Prevention* http://www.cdc.gov/vhf/ebola/outbreaks/2014-west-africa/case-counts.html (2016).
2. Kanapathipillai, R. *et al.* Ebola vaccine--an urgent international priority. *N. Engl. J. Med.* **371**, 2249–2251 (2014).
3. Henao-Restrepo, A.M. *et al.* Efficacy and effectiveness of an rVSV-vectored vaccine expressing Ebola surface glycoprotein: interim results from the Guinea ring vaccination cluster-randomised trial. *Lancet* **386**, 857–866 (2015).
4. Krause, P.R. Interim results from a phase 3 Ebola vaccine study in Guinea. *Lancet* **386**, 831–833 (2015).
5. Marzi, A., Feldmann, F., Geisbert, T.W., Feldmann, H. & Safronetz, D. Vesicular stomatitis virus-based vaccines against Lassa and Ebola viruses. *Emerg. Infect. Dis.* **21**, 305–307 (2015).
6. Marzi, A. *et al.* EBOLA VACCINE. VSV-EBOV rapidly protects macaques against infection with the 2014/15 Ebola virus outbreak strain. *Science* **349**, 739–742 (2015).
7. Rampling, T. *et al.* A monovalent chimpanzee adenovirus Ebola vaccine—preliminary report. *N. Engl. J. Med.* **374**, 1635–1646 (2016).
8. Regules, J.A. *et al.* A recombinant vesicular stomatitis virus Ebola vaccine—preliminary report. *N. Engl. J. Med.* http://dx.doi.org/10.1056/NEJMoa1414216 (2015).
9. Tapia, M.D. *et al.* Use of ChAd3-EBO-Z Ebola virus vaccine in Malian and US adults, and boosting of Malian adults with MVA-BN-Filo: a phase 1, single-blind, randomised trial, a phase 1b, open-label and double-blind, dose-escalation trial, and a nested, randomised, double-blind, placebo-controlled trial. *Lancet Infect. Dis.* **16**, 31–42 (2016).
10. Jones, S.M. *et al.* Live attenuated recombinant vaccine protects nonhuman primates against Ebola and Marburg viruses. *Nat. Med.* **11**, 786–790 (2005).
11. Dye, J.M. *et al.* Postexposure antibody prophylaxis protects nonhuman primates from filovirus disease. *Proc. Natl. Acad. Sci. USA* **109**, 5034–5039 (2012).
12. Holtsberg, F.W. *et al.* Pan-ebolavirus and pan-filovirus mouse monoclonal antibodies: protection against Ebola and Sudan viruses. *J. Virol.* **90**, 266–278 (2016).
13. Marzi, A. *et al.* Antibodies are necessary for rVSV/ZEBOV-GP-mediated protection against lethal Ebola virus challenge in nonhuman primates. *Proc. Natl. Acad. Sci. USA* **110**, 1893–1898 (2013).
14. Wilson, J.A. *et al.* Epitopes involved in antibody-mediated protection from Ebola virus. *Science* **287**, 1664–1666 (2000).
15. Matassov, D. *et al.* Vaccination with a highly attenuated recombinant vesicular stomatitis virus vector protects against challenge with a lethal dose of Ebola virus. *J. Infect. Dis.* **212** (Suppl. 2), S443–S451 (2015).
16. Blaney, J.E. *et al.* Antibody quality and protection from lethal Ebola virus challenge in nonhuman primates immunized with rabies virus based bivalent vaccine. *PLoS Pathog.* **9**, e1003389 (2013).
17. Wong, G. *et al.* Immune parameters correlate with protection against Ebola virus infection in rodents and nonhuman primates. *Sci. Transl. Med.* **4**, 158ra146 (2012).
18. Ruibal, P. *et al.* Unique human immune signature of Ebola virus disease in Guinea. *Nature* **533**, 100–104 (2016).
19. Cohen, J. & Enserink, M. Clinical trials. Ebola vaccines face daunting path to approval. *Science* **349**, 1272–1273 (2015).
20. Krause, P.R., Cavaleri, M., Coleman, G. & Gruber, M.F. Approaches to demonstration of Ebola virus vaccine efficacy. *Lancet Infect. Dis.* **15**, 627–629 (2015).
21. Khurana, S. *et al.* Vaccines with MF59 adjuvant expand the antibody repertoire to target protective sites of pandemic avian H5N1 influenza virus. *Sci. Transl. Med.* **2**, 15ra5 (2010).
22. Khurana, S. *et al.* Antigenic fingerprinting of H5N1 avian influenza using convalescent sera and monoclonal antibodies reveals potential vaccine and diagnostic targets. *PLoS Med.* **6**, e1000049 (2009).
23. Khurana, S. *et al.* MF59 adjuvant enhances diversity and affinity of antibody-mediated immune response to pandemic influenza vaccines. *Sci. Transl. Med.* **3**, 85ra48 (2011).
24. Flyak, A.I. *et al.* Cross-reactive and potent neutralizing antibody responses in human survivors of natural Ebolavirus infection. *Cell* **164**, 392–405 (2016).
25. Davidson, E. *et al.* Mechanism of binding to Ebola virus glycoprotein by the ZMapp, ZMAb, and MB-003 cocktail antibodies. *J. Virol.* **89**, 10982–10992 (2015).
26. Murin, C.D. *et al.* Structures of protective antibodies reveal sites of vulnerability on Ebola virus. *Proc. Natl. Acad. Sci. USA* **111**, 17182–17187 (2014).
27. Lee, J.E. *et al.* Structure of the Ebola virus glycoprotein bound to an antibody from a human survivor. *Nature* **454**, 177–182 (2008).
28. Yang, J. *et al.* The I-TASSER Suite: protein structure and function prediction. *Nat. Methods* **12**, 7–8 (2015).
29. Geisbert, T.W. *et al.* Single-injection vaccine protects nonhuman primates against infection with marburg virus and three species of Ebola virus. *J. Virol.* **83**, 7296–7304 (2009).
30. Chung, K.Y. *et al.* ISCOMATRIX™ adjuvant promotes epitope spreading and antibody affinity maturation of influenza A H7N9 virus-like particle vaccine that correlate with virus neutralization in humans. *Vaccine* **33**, 3953–3962 (2015).
31. Nicholson, K.G. *et al.* Safety and antigenicity of non-adjuvanted and MF59-adjuvanted influenza A/Duck/Singapore/97 (H5N3) vaccine: a randomised trial of two potential vaccines against H5N1 influenza. *Lancet* **357**, 1937–1943 (2001).
32. Jackson, L.A. *et al.* Effect of varying doses of a monovalent H7N9 influenza vaccine with and without AS03 and MF59 adjuvants on immune response: a randomized clinical trial. *J. Am. Med. Assoc.* **314**, 237–246 (2015).
33. Mulligan, M.J. *et al.* Serological responses to an avian influenza A/H7N9 vaccine mixed at the point-of-use with MF59 adjuvant: a randomized clinical trial. *J. Am. Med. Assoc.* **312**, 1409–1419 (2014).
34. Fuentes, S., Coyle, E.M., Beeler, J., Golding, H. & Khurana, S. Antigenic fingerprinting following primary RSV infection in young children identifies novel antigenic sites and reveals unlinked evolution of human antibody repertoires to fusion and attachment glycoproteins. *PLoS Pathog.* **12**, e1005554 (2016).
35. Gitlin, A.D. *et al.* Humoral immunity. T cell help controls the speed of the cell cycle in germinal center B cells. *Science* **349**, 643–646 (2015).
36. McHeyzer-Williams, L.J., Milpied, P.J., Okitsu, S.L. & McHeyzer-Williams, M.G. Class-switched memory B cells remodel BCRs within secondary germinal centers. *Nat. Immunol.* **16**, 296–305 (2015).
37. Khurana, S. *et al.* DNA priming prior to inactivated influenza A(H5N1) vaccination expands the antibody epitope repertoire and increases affinity maturation in a boost-interval-dependent manner in adults. *J. Infect. Dis.* **208**, 413–417 (2013).
38. Ledgerwood, J.E. *et al.* Prime-boost interval matters: a randomized phase 1 study to identify the minimum interval necessary to observe the H5 DNA influenza vaccine priming effect. *J. Infect. Dis.* **208**, 418–422 (2013).
39. Halliley, J.L. *et al.* High-affinity H7 head and stalk domain-specific antibody responses to an inactivated influenza H7N7 vaccine after priming with live attenuated influenza vaccine. *J. Infect. Dis.* **212**, 1270–1278 (2015).
40. Talaat, K.R. *et al.* A live attenuated influenza A(H5N1) vaccine induces long-term immunity in the absence of a primary antibody response. *J. Infect. Dis.* **209**, 1860–1869 (2014).

ONLINE METHODS

Sera samples and monoclonal antibodies. Monoclonal antibodies (MAbs) and recombinant EBOV GP used in this study were purchased from IBT Bioservices Inc. Cross-reactive conformation-dependent neutralizing and protective human MAb 289 and MAb 324 from EBOV survivors were obtained from J. Crowe[24]. Phase 1, double-blind, placebo-controlled, dose-escalation trials with staggered enrollment were designed across three dose levels as outlined in Regules *et al.*[8]. Briefly, the rVSVΔG-ZEBOV-GP vaccine consisting of the rVSV strain Indiana and the glycoprotein of the EBOV Kikwit 1995 strain replacing the gene encoding the VSV envelope glycoprotein was administered at 3 million, 20 million or 100 million PFU in the form of a 1-mL injection in the deltoid muscle of healthy adult men and women according to protocols approved by the institutional review board at the US National Institutes of Health NIAID site. Written informed consent was obtained from all the volunteers before enrollment. Within each dosing cohort, 10 received active vaccine and 3 received a saline placebo. Serum samples from each individual were collected before vaccination (day 0), after the first vaccination (day 28), after the second vaccination (days 42 and 56), and on day 84 and day 180 (ClinicalTrials.gov number NCT02280408). Samples were anonymous, and permission to test these deidentified samples in different antibody assays was obtained from the US Food and Drug Administration's Research Involving Human Subjects Committee (FDA-RIHSC) under exemption protocol #15-0B; all assays done fell within the permissible usages in the original consent.

PsVN assay. Pseudovirion neutralization assay (PsVNA) against the homologous Zaire-Kikwit strain glycoprotein was performed as described previously[8].

GFPDL construction. cDNAs complementary to the envelope glycoprotein–encoding gene of EBOV Mayinga or Kikwit strain were chemically synthesized and used for cloning. A gIII display-based phage vector, fSK-9-3, where the desired polypeptide can be displayed on the surface of the phage as a gIII-fusion protein, was used. Purified DNA containing Ebola *GP* was digested with DNase I to obtain gene fragments of 50–1,000 bp and used for GFPDL construction as described previously[22,23]. As the phage libraries were constructed from the whole gene, they potentially display all possible known or unknown viral protein segments ranging in size from 15 to 350 amino acids as fusion proteins on the surface of the bacteriophage.

Adsorption of polyclonal human sera on EBOV GFPDL phages and residual reactivity to EBOV GP. Prior to panning of GFPDL, 500 µl tenfold-diluted serum antibodies from post-vaccination pooled human sera (n = 10 each from the 20-million-PFU and 100-million-PFU groups; 5 µl serum from each vaccine to obtain a tenfold dilution for the pooled sera) were adsorbed by incubation in EBOV GFPDL phage-coated petri dishes. To ascertain residual antibody specificity, an ELISA was performed in wells coated with 200 ng/100 µl recombinant EBOV GP. After blocking with 20 mM PBS, pH 7.4, containing 0.05% Tween-20 (PBST) containing 2% milk, serial dilutions of human serum (with or without adsorption) in blocking solution were added to each well and incubated for 1 h at room temperature (RT) before addition of 5,000-fold diluted HRP-conjugated goat anti-human IgA + IgG + IgM antibody and developed by 100 µl *o*-phenylenediamine dihydrochloride (OPD) substrate solution. Absorbance was measured at 490 nm.

Affinity selection of EBOV GP GFPDL phages with rVSVΔG-ZEBOV-GP post-vaccination polyclonal human sera. Prior to panning of GFPDL with polyclonal serum antibodies, serum components that could nonspecifically interact with phage proteins were removed by incubation in UV-killed M13K07 phage-coated petri dishes. Equal volumes of pooled polyclonal human sera from each cohort were used for each round of GFPDL panning. All samples in each group (N = 10) were pooled for GFPDL analysis. Subsequent GFPDL affinity selection was carried out in solution (with protein A/G) as previously described[22,23]. GFPDL affinity selection experiments were performed in quadruplicate (two independent experiments by two different investigators, who were blinded to sample identity) and showed similar numbers of phage clones and epitope repertoires. Additional antibody epitope repertoire analysis was performed using individual post-vaccination sera with similar neutralization titers from 20-million- and 100-million-PFU dose groups using IgA-, IgG- and IgM-specific capture beads to further define the fine epitope specificity of these antibodies in the individual sera using EBOV Kikwit GP GFPDL. A model for the complete Zaire strain GP generated using I-TASSER[28] was used to represent the antigenic sites on the structure. The crystal structure of Ebola GP (PDB 3CSY) was used as a reference[27].

Binding of rVSVΔG-ZEBOV-GP-vaccinated human sera to recombinant GP and off-rate measurements by surface plasmon resonance (SPR). Steady-state equilibrium binding of pre- and post-vaccination human polyclonal sera from every individual in the study was monitored at 25 °C using a ProteOn surface plasmon resonance (Bio-Rad). The purified recombinant GP was coupled to a GLC sensor chip via amine coupling with either 100 or 500 resonance units (RU) in the test flow channels. The protein density on the chip was optimized to measure only monovalent interactions independent of the antibody isotype. Samples of 300 µl freshly prepared sera at tenfold and 100-fold dilution BSA-PBST buffer (PBS, pH 7.4, with Tween-20 and BSA) were injected at a flow rate of 50 µl/min (240 s contact duration) for association, and disassociation was performed over a 1,200-s interval. Responses from the protein surface were corrected for the response from a mock surface and for responses from a buffer-only injection. SPR was performed with serially diluted sera (tenfold and 100-fold dilutions) of each sample in this study such that the SPR signal of the samples between 5 to 100 RU was used for further quantitative analysis. The maximum resonance units (max RU) data were calculated by multiplying the observed RU signal with the dilution factor for each serum sample to provide the data for an undiluted serum sample. Antibody isotype analysis for the GP-bound antibodies in post-vaccination polyclonal sera was performed using SPR. Total antibody binding and isotype analysis were calculated with Bio-Rad ProteOn manager software (version 3.0.1). All SPR experiments were performed twice, and the researchers performing the assay were blinded to sample identity. In these optimized SPR conditions, the variation for each sample in duplicate SPR runs was <6%.

Antibody off-rate constants, which describe the stability of the complex, i.e., the fraction of complexes decaying per second, were determined directly from the post-rVSVΔG-ZEBOV-GP-vaccination human polyclonal sera sample interaction with rGP protein using SPR (as described above) and calculated using the Bio-Rad ProteOn manager software for the heterogeneous sample model.

Purification of IgG and IgM antibodies from the post-vaccination sera. Fivefold-diluted post-second-vaccination sera were added to anti-human IgG or anti-human IgM immune-affinity resin and incubated for 1 h at RT on an end-to-end shaker before washing and purification of bound antibodies. The antibodies were eluted by 4 M magnesium chloride in 10 mM Tris (pH 7), followed by desalting. The purified IgG and IgM antibodies were normalized by volume to original serum concentrations and tested for GP binding then isotyped using anti-human IgG and anti-human IgM secondary antibodies in SPR to confirm the purity of each antibody isotype preparation. The purified IgG and IgM antibodies were subjected to virus-microneutralization assay.

Statistical analyses. The statistical significance of group differences was determined by ordinary one-way ANOVA and Bonferroni's multiple-comparisons method. $P < 0.05$ was considered significant with a 95% confidence interval. Correlations were calculated with the Pearson method, and P values for correlation were calculated by two-tailed test.

Data availability. The data sets generated during and/or analyzed during the study are available from the corresponding author upon reasonable request.

doi:10.1038/nm.4201